

Emission geometry of pulsar J0631+1036

Mateus M. Teixeira & Joanna M. Rankin

*Department of Physics, University of Vermont, Burlington, VT 05405**

Originally drafted 2011 09 22

ABSTRACT

Radio pulsar J0631+1036 presents a remarkably clear example of a rare four-component profile, and on closer study almost every aspect of it is strange or difficult to understand: the spacing of its four components; its evolution over the available 3 octaves; and the apparent large aberration/retardation indicated by its linear polarization-angle traverse. Given the broad success of the core/double-cone geometric model in describing pulsar profiles, we attempt such an analysis for J0631+1036. The values resulting from application of this model for the magnetic colatitude α and sightline impact angle β are not implausible; however, overall the model appears to fail for several different reasons. We eager to understand how it is that the double conal beam model fails here when it work so well for so many other radion pulsars.

Key words: miscellaneous – aberration/retardation – emission height – emission geometry – methods: – data analysis – pulsars: general, individual (J0631+1036)

1 INTRODUCTION

The highly unusual pulse profile of pulsar J0631+1036 in Figure 1 (top) consists of two pairs of nearly symmetrical components, all highly linearly polarized at 1400 MHz. Four-component forms are rare in the radio pulsar population, whereas one finds hundreds of triple and scores of five-component profiles. For slower pulsars (rotation periods greater than 100 ms or so), the core-double cone beaming model provides a successful quantitative description for the vast majority of stars (ET VI, ET IX). Triple profiles then usually represent sightline traverses through one cone and the core, whereas five-component profiles reflect both cones and the core. The few available four-component profiles exhibit forms similar to those of five-component pulsars—but absent a central core feature (*e.g.*, B1738–08 in ET VI); also the inner conal component pair is generally weaker. Thus their four components do not usually appear evenly spaced—but rather as leading and trailing pairs. The J0631+1036 21-cm profile is thus striking both because of the near even spacing of its four components and the pronounced relative weakness of its outer component pair.

This is not all: Also striking is the very high fractional linear polarization of the 21-cm. profile in Fig. 1 across almost the full width of the profile. Most radio pulsar profiles are highly linearly polarized, but largely complete polarization is rare. Further, the accompanying polarization position-angle (hereafter PPA) traverse of J0631+1036 is

no less remarkable, sweeping the greater part of the canonical 180° associated with a central sightline geometry, but in a strikingly asymmetric manner. Indeed, the steepest gradient point falls not near the profile center but on its far trailing edge, clearly suggesting that aberration/retardation (hereafter A/R) is a significant factor in its structure.

Finally, the pulsar’s evolution with frequency is also difficult to understand. At 327-MHz (Fig. 1, bottom), the J0631+1036 profile is much broader and has the form of an unresolved double. Much of its width shows large linear polarization, and the steepening of the PPA traverse toward on the trailing side of the profile is visible. Such a profile evolution—that is, broader at longer wavelengths—is an expected aspect of outer conal emission; however, that the emission component number appears to change from one frequency to another—this is virtually unknown and deserves explanation.

PSR J0631+1036 was discovered by Zepka *et al.* (1996), in the course of an Arecibo search targeted at *Einstein* IPC X-ray sources. It has a rotation period P_1 of 0.288 s and a spindown of 1.05×10^{-13} s/s, giving it a large magnetic field (5.6×10^{12} G), acceleration potential (66.9) and rotational energy loss (1.7×10^{35} ergs). The pulsar was also detected at γ -ray energies by the Fermi-LAT Observatory (Weltevrede *et al.* 2010), and Seyffert *et al.* (2011) also discuss its interpretation. Such a high energy-loss rate (indeed, high energy detection!) and acceleration potential suggests that its emission might be core dominated, but nothing about its profile form supports this interpretation. Figure 2 reproduces Zepka *et al.*’s fig. 3, where the pulsar’s polarized profile can be seen at four frequencies between 430 and 2380 MHz.

* Mateus.Teixeira@uvm.edu; Joanna.Rankin@uvm.edu

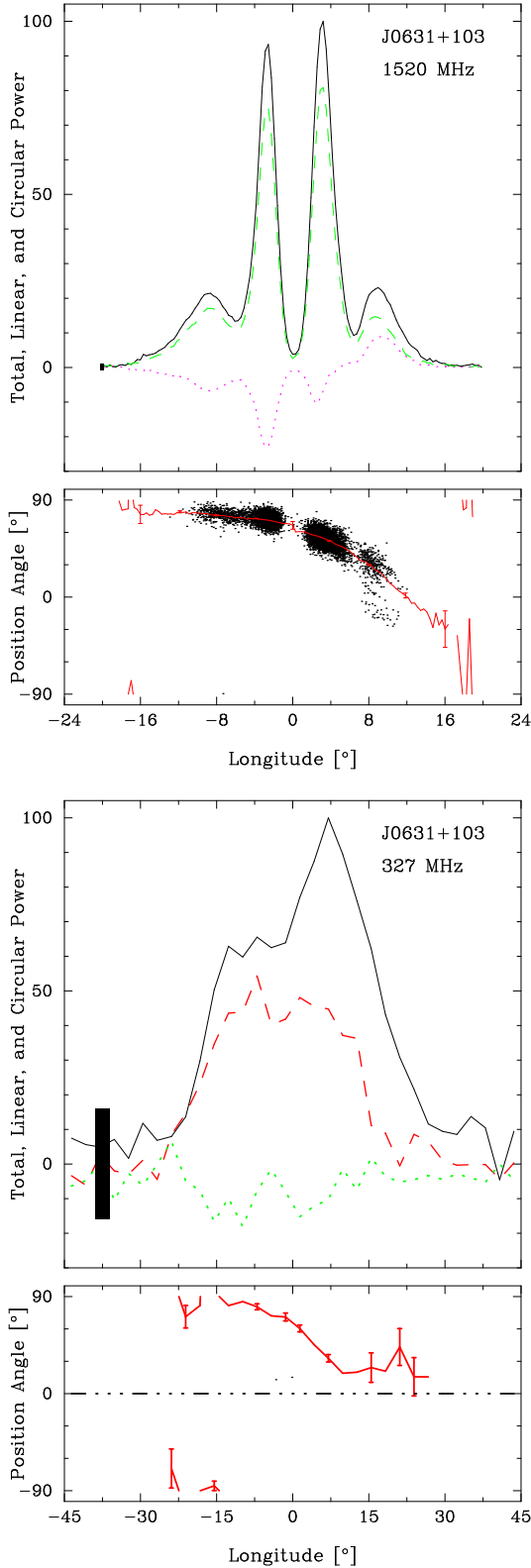


Figure 1. J0631+1036 polarization profiles at 1520 MHz (top) and 327 MHz (bottom); Stokes I (solid), total linear polarization ($L = \sqrt{Q^2 + U^2}$; dashed green) and circular polarization (Stokes V , defined as left-right-hand; dotted magenta) (upper), and the average PPA ($\chi = \frac{1}{2} \tan^{-1}(U/Q)$) (lower). Note the nearly equally spaced four components and the asymmetric PPA traverse of the 1520-MHz profile (top) as well as the greatly larger overall width of the 327-MHz profile (bottom).

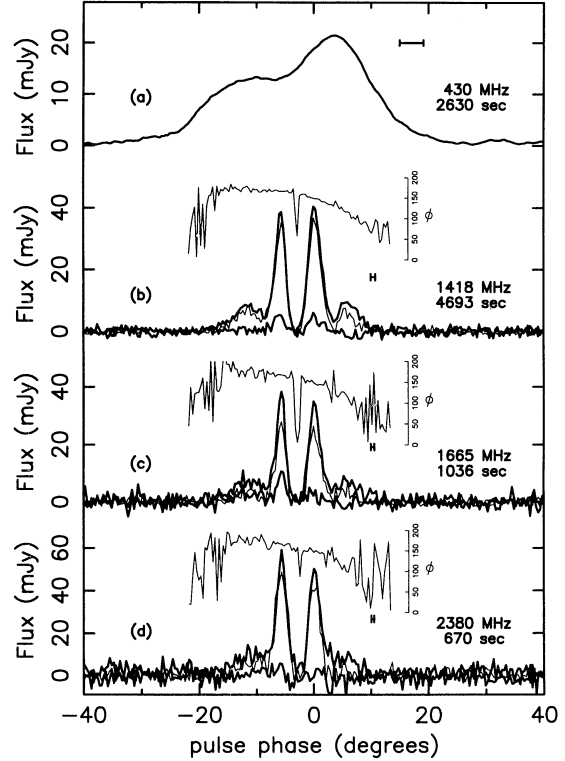


Figure 2. Zepka *et al.*'s (1996) fig. 3 showing the polarized profile forms at three frequencies and a 430-MHz total-power profile.

In this short report we trace the steps we have taken to perform a comprehensive geometric analysis of J0631+1036's emission profiles and then to interpret it. In §II we further discuss the morphological characteristics of the star's average profile as well as its spreading at lower frequencies, so as to define the profile dimensions pertinent to our analysis. §III then presents a quantitative analysis of the star's putative inner and outer conal component geometry after the manner of ET VI, and §IV an overview of the A/R effects in this context. Finally, §V discusses our results.

2 MORPHOLOGY & CONAL SPREADING

The average profile of pulsar J0631+1036 develops remarkably over the three octaves of available observations. At meter wavelengths (*e.g.*, 327 MHz), its total power profile exhibits a conal double (D) configuration (as per the classification in ET I & ET VI), with a full width at half maximum (FWHM) of $\sim 34^\circ$. At L-band by contrast, J0631+1036's average profile develops into a well resolved set of four highly symmetrical components, with near zero emission between the inner pair; see Figure 3. The FWHM measure for the 1520-MHz total power profile is some $\sim 22.5^\circ$, significantly narrower than the low frequency profile, as would be expected for a conal emission geometry—and by using our other profiles at 1170 and 1420 MHz and those of Zepka *et al.* at 430, 1665 and 2380 MHz (23.2, 22.0, 31, 21.5 and 21° , respectively) we were able to assemble the information for modeling in Table 1.

Note that the FWHM values show a progressive increase

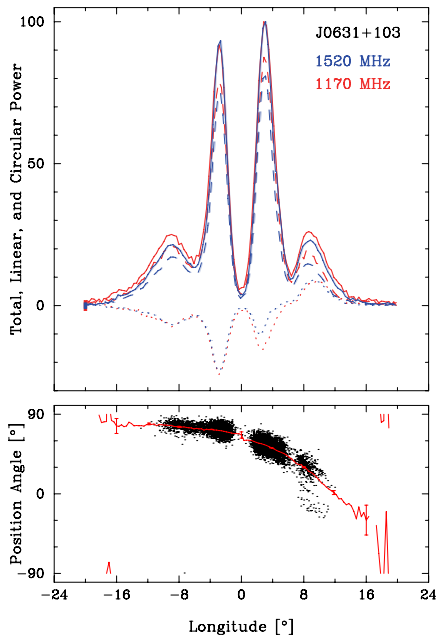


Figure 3. Overlaid average profiles at 1170 MHz (red) and 1520 MHz (blue), including polarimetry information (circular polarization as a dotted curve, linear as dashed), for PSR J0631+1036 (above). The average PPA traverse in the bottom panel corresponds to that of the three combined bands, and is provided for comparison with Figure 1. Note that here as well as in Fig. 2 the amplitudes of the outer component pair increase with wavelength.

with wavelength as would be expected for an outer cone. The outer-edge depolarization, marked in clear contrast to the overall large fractional linear polarization ($>70\%$), also supports this interpretation. FWHM values for the inner component pair, though visible only at L band and higher, change little with frequency, hovering around 8.3° as would be expected for an inner cone. Moreover, the outer-conal component pair appears to have a steeper spectrum than the inner pair, suggesting that the meter-wavelength profiles are dominated by the outer conal emission.¹ Furthermore, the large linear polarization (at both high and low frequency) supports accurate PPA determination, and the L-band profiles define the PPA traverse best, especially on the trailing edge of the profile where the inflection or steepest gradient (SG) point appears to fall.

Figure 4 then shows the results of a single-vector model (hereafter SVM) fit to the pulsar’s PPA traverse at 1520 MHz. The four-parameter fit fixes the longitude origin at the SG point of the traverse. It also determines nominal values of magnetic colatitude α and sightline impact angle β . However, these latter values are typically 99% correlated, so it is the PPA slope $R_{PA} [= \sin \alpha / \sin \beta]$ at the SG point

¹ No profile at 600 MHz or so seems to exist, but such a profile could show this aspect of the star’s profile evolution clearly.

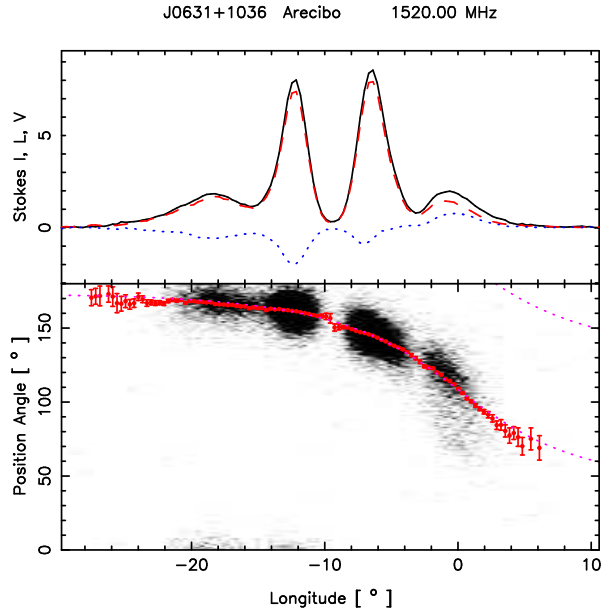


Figure 4. J0631+1036 L-band profile and PPA fit at 1520 MHz (dotted magenta line, bottom panel). The longitude origin is taken at the fitted PPA inflection point and the fitted traverse corresponds to $\alpha = 36.5^\circ$ and $\beta = -5.0^\circ$, in the convention of ET VI. However, the latter values are very highly correlated, so it is central slope $R_{PA} [= \sin \alpha / \sin \beta]$ of $-6.8 \pm 0.2^\circ/^\circ$ that is significant.

that is significant and well determined (see also ET IX). This value is $-6.8 \pm 0.2^\circ/^\circ$.

As a whole, the morphological characteristics of J0631+1036 suggest a pulsar whose emission features largely place it in the conal quadruple class (cQ) (ET VI).

3 QUANTITATIVE GEOMETRY

The most accurate and consistent estimates of a radio pulsar’s emission geometry—that is, its magnetic colatitude α and sightline impact angle β —come from using *both* the angular width information of its profile and the sightline-path information in its PPA traverse. This was the method used in ET VI (Rankin 1993) wherein the bulk of the population with then well measured polarization profiles were found to exhibit a core/double-cone structure with a half-power core width of $2.45^\circ/P^{-1/2}$ and outside half-power conal radii of $4.3^\circ P^{-1/2}$ and $5.8^\circ P^{-1/2}$ (all at 1 GHz), respectively.² And these conal radii then imply *characteristic* emission heights of some 130 and 220 km, respectively.³

² Lyne & Manchester (1988) carried out a similar geometric study and came to many of the same conclusions. However, they also identified a group of some 50 so-called ‘partial cone’ pulsars that appeared not to exhibit core/conal structure. Reinvestigation of this population using new observations, however, has shown that the vast majority exhibit a core/double-cone profile structure with the above dimensions (ET IX).

³ Such *characteristic* emission heights are not to be confused with actual, physical emission heights. In the ET VI context, computation of emission heights entails association of the conal emission outer boundary (for both inner and outer cones!) with the ‘last

Table 1. Double Cone Emission Geometry Model for Pulsar J0631+1036

$\alpha(^{\circ})$	Rpa($^{\circ}/^{\circ}$)	f(GHz)	W1($^{\circ}$)	$\rho 1(^{\circ})$	$\beta/\rho 1$	W2($^{\circ}$)	$\rho 2(^{\circ})$	$\beta/\rho 2$	h1(km)	h2(km)
60	-6.8	2380	8.3	8.1	-.90	21.0	11.4	-.64	125	249
		1665	8.3	8.1	-.90	21.5	11.5	-.63	125	256
	$\beta(^{\circ})$	1520	8.3	8.1	-.90	22.0	11.7	-.63	125	263
	-7.3	1420	8.3	8.1	-.90	22.5	11.9	-.62	125	270
		1170	8.3	8.1	-.90	23.2	12.1	-.60	125	281
		430	—	—	—	31	14.8	-.49	—	420
		327	—	—	—	34	15.9	-.46	—	485

Pulsar J0631+1036’s profile long seemed so unusual and strange to us that we did not think to view it as that of an inner and outer conal component pair. However, as we have seen in the foregoing section, the actual properties of this profile—its frequency evolution, edge depolarization and PPA traverse—all in fact appear compatible with this interpretation. What remains then is to ask whether such a geometry is consistent quantitatively. No core feature is discernible at any frequency for this pulsar, so we have no independent means of estimating the pulsar’s magnetic colatitude. However, we can ask where there is any value of α such that the two putative emission cones have the expected dimensions.

Table 1 gives such a double-cone geometric model for J0631+1036. The model value of α , the PPA sweep rate R_{PA} and β are shown at the extreme left of the table. Column 3 gives the frequencies for which inner and outer half-power widths can be determined, and these measured values appear in columns 4 and 7, respectively. The respective conal radii are computed in columns 5 and 8 according to ET VI eq. (4) and the emission heights in columns 10 and 11 per eq. (6). Only for this last computation is the pulsar’s rotation period P_1 (0.288 s) used to estimate the angular size of the star’s polar cap so that magnetic-polar colatitudes can be related to *characteristic* emission heights.

More or less reasonable conal dimensions and emission heights can be obtained using the model in Table 1 for α values between about 50 and 60°. For α near the upper value, the inner cone exhibits its expected radius and emission height, and for the lower value the outer cone assumes a radius such that the model 1-GHz *characteristic* emission height is about the expected 220 km. The issue is that an intermediate α value gives a height unfamiliarly low for the inner cone and high for the outer cone. This situation is very unusual and suggests that a double cone model is somehow fundamentally the wrong geometry for J0631+1036.

open” field line. Clearly this is an implausible circumstance physically; however, its use provides a consistent outer boundary for emission along the edges of the polar flux tube. Emission heights computed using the profile peaks would be more physical, and in fact such values are usually 2-3 times greater and agree better with *physical* emission heights now estimated most generally using A/R; see below.

4 A/R EMISSION-HEIGHT ESTIMATION

As we saw in the J0631+1036 profiles above, the star’s PPA traverse is so SVM-like and its SG point so dramatically delayed with respect to the profile center that the situation seems almost to scream out for A/R analysis. Not so fast, however! The physical basis and practical application of A/R analysis was first developed by Blaskiewicz, Cordes & Wasserman (1991) (hereafter BCW), but only over the last decade or so has it found wide application and provided increasingly consistent results. Fundamental to all A/R analyses is reliable determination of a profile center which can be interpreted as the longitude of the magnetic axis. Such interpretations have followed one of two courses: a) taking the midpoint between two conal components as indicative of the magnetic axis longitude (BCW), and b) taking the center of a core component as such a center [Malov & Su-leymanova (1998) and later Gangadhara & Gupta (2001), hereafter G&G]. The unusual “failure” of the double cone model for J0631+1036 above, however, gives us pause. The star’s four components may not represent inner and outer conal component pairs. However, their striking symmetry remains, and it is hard to understand how the longitude of the magnetic axis could fall at any other point than at the centers of the two pairs.

So emboldened, we have conducted an A/R analysis of the former type. However, in terms of computations, all are the same, and the values in Table 2 are similar to tables in previous such efforts in G&G, Srothlik & Rankin (2005), Force & Rankin (2010) or Mitra & Rankin (2010) and are corrected as advised by Dyks, Rudak, & Harding (2004). ϕ_l^i and ϕ_t^i are the respective leading and trailing longitudes of the centers of one or the other component pairs; ν^i is the computed center of the pair; ρ^i is the computed radius of the emission cone; and r_{em}^i and s_L^i give the physical emission height and relative polar cap annulus, respectively.

Here again the results are interesting but strange. The computed physical emission heights for the inner and outer “cones” are indistinguishable within their errors. The values near 1130 km are very large for an outer cone at about 1 GHz (500-600 km) would be more typical), and we have never seen a case where putative inner and outer conal emission occurred at essentially the same physical height. Moreover, the emission annuli traced down to the polar cap—hardly 1/3 or the way out from the magnetic axis—are very unlike any such A/R results for inner and outer cones we have seen before. All this suggests again that the double-cone model as applied to J0631+1036 is somehow fundamentally incorrect.

Table 2. Aberration/retardation analysis results for PSR J0631+1036.

Cone	ϕ_l^i ($^\circ$)	ϕ_t^i ($^\circ$)	ν^i ($^\circ$)	ρ^i ($^\circ$)	r_{em}^i (km)	s_L^i
outer	-18.5 ± 0.2	-0.7 ± 0.2	-9.6 ± 0.2	7.0 ± 0.1	1151 ± 17	0.28 ± 0.01
inner	-12.3 ± 0.1	-6.5 ± 0.1	-9.4 ± 0.1	5.3 ± 0.1	1127 ± 8	0.21 ± 0.01

5 DISCUSSION

Pulsar J0631+1036 appears to provide a very interesting instance in which the core/double cone model of radio pulsar emission geometry fails to give an adequate description. Not only does the model fail to give the observed ratio of (putative) conal emission radii, but it would suggest that the (putative) inner and outer cones are emitted at the same physical height. Such results have not been seen before the in the pulsar population to which these ideas have been applied.

While our attempts to model the J0631+1036 geometry have been confined entirely to the radio region, we note that great interest in the pulsar was generated following its detection in γ rays by Fermi LAT (Weltevrede *et al.* 2010). As in so many other such cases, the radio and γ -ray profiles could not be more different, the former being narrow and symmetrical and the latter broad seemingly misaligned. Great effort, however, has recently been expended in understanding the beaming characteristics of pulsars in the γ -ray region, and even this discovery paper was able to argue that “ α was close to 90° ” and $\beta \sim -4^\circ$. Seyffert *et al.* (2011) provide two models for the pulsar’s γ -ray emission region—the outer gap (OG) and two-pole caustic (TPC) models. In both models, the emission originates from gaps along the last open field lines, the difference being that, in the OG model, emission originates above the null charge surface and interior to the last open field line, whereas the TPC gap is taken at the stellar surface. The OG model yields α and β values of $74 \pm 5^\circ$ and $-6 \pm 2^\circ$, respectively. The TPC model yields results of $71 \pm 6^\circ$ and $-5 \pm 3^\circ$. Clearly these results are neither entirely incompatible nor obviously more accurate than our effort above. We see little basis for deciding between them.

Finally, it is interesting to speculate about the nature of pulsar J0631+1036’s unusually large fractional linear polarization. In an OPM sense, its emission is nearly unimodal—that is, any secondary polarization-mode power must be at least roughly 10 times weaker across the profile than the primary mode power (except on the extreme edges of the outer component pair where some edge depolarization is seen). Following the Johnston & Weisberg (2006) reasoning, this suggests that the pulsar’s emission occurs above the polarization limiting height—that is, where the magnetospheric plasma is so tenuous that the normal propagation modes are essentially the same as those in vacuum. Here, the 1130-km putative physical emission height corresponds to about 8% of the velocity-of-light cylinder radius. The A/R analysis would seem to support this conjecture in that 1-GHz physical emission heights for outer-cone emission (that is much less linearly polarized) tend to be no more than about 500 kms.

Acknowledgments: Portions of this work were carried out with support from US National Science Foundation Grant AST 08-07691. Arecibo Observatory was until recently operated by Cornell University under contract to the US NSF and is now managed by a consortium led by SRI under a similar NSF contract. This work used the NASA ADS system.

REFERENCES

- Blaskiewicz, M., Cordes, J.M., Wassermann, I. 1991, *Ap.J.*, 370, 643
- Dyks, J., Rudak, B., & Harding, A. K. 2004, *Ap.J.*, 607, 939
- Force, M. M., & Rankin, J. M. 2010, *MNRAS*, 406, 237
- Gangadhara R. T., & Gupta Y. 2001, *Ap.J.*, 555, 31
- Johnston, S., & Weisberg, J. M. 2006, *MNRAS*, 368, 1856
- Malov, I. F., & Suleymanova, S.A. 1998, *Astron. Rep.*, 42, 388
- Mitra, D., Rankin, J. M. 2010, *Ap.J.*, 727, 92 (ET IX)
- Rankin, J. M. 2010, *Ap.J.*, 274, 333 (ET I)
- Rankin, J.M. 1993, *Ap.J.*, 405, 285 and *A&A Suppl.*, 85, 145 (ET VI)
- Seyffert, A. S., Venter, C., de Jager, O. C., Harding, A. K. 2011, arXiv:1105.4094v1
- Sroostlik, Z., & Rankin, J. M. 2005, *MNRAS*, 362, 1121
- Weltevrede, P., et al. 2010, *Ap.J.*, 708, 1426
- Zepka, A., Cordes, J. M., Wasserman, I., & Lundgren, S. C. 1996, *Ap.J.*, 456, 305